

# Kinetic Freeze-out and Radial Flow in 11.6 A GeV Au+Au Collisions

Harald Dobler<sup>a</sup>, Josef Sollfrank<sup>a</sup>, Ulrich Heinz<sup>b,\*</sup>

<sup>a</sup>*Institut für Theoretische Physik, Universität Regensburg, D-93040 Regensburg, Germany*

<sup>b</sup>*Theoretical Physics Division, CERN, CH-1211 Geneva 23, Switzerland*

(September 3, 2018)

We study the kinetic freeze-out conditions of hadrons in Au+Au collisions at 11.6 A GeV/c using different parametrizations of an expanding thermal fireball. We take into account the available double differential momentum spectra of a variety of particle species, covering a large fraction of the total momentum space. The overall fit to the data is very good and indicates a relatively low kinetic freeze-out temperature of about 90 MeV with an average transverse expansion velocity at midrapidity of about 0.5  $c$ .

PACS numbers: 25.75.-q, 25.75.Ld, 24.10.Pa

When studying the nuclear phase diagram in extreme regions of temperature and density with heavy-ion collisions one is faced with the difficulty that, due to the limited size and strong dynamics of the fireballs created in such collisions, full (global) thermodynamic equilibrium and the thermodynamic (infinite volume) limit can never be reached. The best one can hope for is a state of *local* thermal equilibrium in a hydrodynamically expanding environment, with thermodynamic homogeneity volumes of several 100 to 1000 fm<sup>3</sup> [1]. If sufficient local equilibration is achieved one can try to extrapolate from the experimental findings to the thermodynamic limit. The most exciting prospect of such an endeavour is the experimental confirmation of a deconfinement phase transition in hot and dense nuclear matter [2].

In order to reach this goal an extensive experimental program has been launched studying heavy-ion collisions at various beam energies. The onset of a new phase of nuclear matter would probably be most clearly seen in a study of different observables as functions of beam energy. For this purpose it is necessary to carefully analyze the data at all available beam energies. Here we present a study of the experimental particle spectra from Au+Au collision at a beam momentum of 11.6 A GeV/c measured by several groups [3–5] at the Brookhaven AGS. The goal is to find a simple, but realistic parametrization of the freeze-out stage in these collisions. The extracted freeze-out parameters, especially the temperature and the mean transverse flow velocity, will be compared with other collision systems and with collisions at different energies.

---

\*On leave from Institut für Theoretische Physik, Universität Regensburg; email address: Ulrich.Heinz@cern.ch

This should help to understand the gross features of the collision dynamics at ultrarelativistic energies.

For the description of particle production we start from the formalism of Cooper and Frye [6] which describes the single-particle spectrum as an integral over a freeze-out hypersurface, thus summing the contributions from all space-time points at which the particles decouple from the fireball:

$$E \frac{d^3N}{d^3p} = \frac{g}{(2\pi)^3} \int_{\Sigma_f} p^\mu d\sigma_\mu(x) f(x, p). \quad (1)$$

Here  $g$  is the degeneracy factor and  $f(x, p)$  the momentum distribution at space-time point  $x$ . In thermal models one uses for  $f(x, p)$  a thermal equilibrium distribution and determines  $\Sigma_f$  by a freeze-out criterium for thermal decoupling [7]. For the low temperatures discussed below the Boltzmann approximation is sufficient, but we allow for a space-time dependence of the temperature  $T$ , the chemical potential  $\mu$ , and the flow velocity  $u^\mu$ :

$$f(x, p) = \exp\left(-\frac{p \cdot u(x) - \mu(x)}{T(x)}\right). \quad (2)$$

Our choice of the geometry of the freeze-out surface  $\Sigma_f$  and of the space-time dependence of the parameters reflects a compromise between relative simplicity of the model and importance of its dynamical ingredients. Focussing on central collisions, we assume azimuthal symmetry of the spatial geometry and momentum distributions. We further assume boost-invariant collective dynamics along the longitudinal ( $z$ ) direction [8]. This was shown before [9] to give a better representation of the measured rapidity spectra than a static “Hagedorn” fireball. Also, a static fireball yields a much stronger rapidity dependence of the transverse slope parameters,  $T_{\text{slope}} = T / \cosh(y - y_{\text{mid}})$ , than observed [3–5]. The assumption of longitudinal Bjorken flow suggests to use longitudinal proper time  $\tau = \sqrt{t^2 - z^2}$  and space-time rapidity  $\eta = \text{Arctanh}(z/t)$  as suitable variables in the  $t$ - $z$ -plane; the transverse radial coordinate is denoted by  $r_\perp$ . Midrapidity is defined to be at  $\eta = 0$ . Longitudinal boost-invariance of the flow field is implemented by the choice  $u^\mu(x) = \gamma(1, v_\perp(x)e_r, v_z(x))$  with  $v_z(\tau, r_\perp, \eta) = \tanh \eta$ . In transverse direction we take a linear flow rapidity profile,  $\tanh v_\perp = \rho(\eta) \frac{r_\perp}{R_0}$ , where  $R_0$  is the transverse radius at midrapidity and  $\rho(\eta)$  will be specified below.

The geometry of the freeze-out hypersurface  $\Sigma_f$  is fixed as follows: In the time direction we take a surface of

constant proper time,  $\tau = \tau_0$ . In  $\eta$ -direction the freeze-out volume extends only to a maximum space-time rapidity  $\eta_{\max}$ ; this breaks longitudinal boost-invariance, as required by the finite available total energy. In the transverse direction the boundary is given by  $R(\eta)$  which may depend on  $\eta$ . We consider two choices:

$$R(\eta) = R_0 \cdot \Theta(\eta_{\max}^2 - \eta^2), \quad (3)$$

$$R(\eta) = R_0 \cdot \sqrt{1 - \frac{\eta^2}{\eta_{\max}^2}}. \quad (4)$$

The first choice (3) describes a cylindrical fireball in the  $\eta$ - $r_{\perp}$ -space. For 200 A GeV S+S collisions at the SPS such a picture was shown to work well [7], but for the lower AGS beam energy this can no longer be expected. An elliptic or cigar shape as given in Eq. (4) should be more appropriate [10].

Having specified the freeze-out geometry and the distribution function (2) at freeze-out we obtain the following thermal single-particle spectrum:

$$\begin{aligned} \frac{dN}{m_T dm_T dy} &= \frac{g}{2\pi} m_T \tau_0 \int_{-\eta_{\max}}^{+\eta_{\max}} d\eta \cosh(y - \eta) \\ &\times \int_0^{R(\eta)} r_{\perp} dr_{\perp} I_0\left(\frac{p_T \sinh \rho(r_{\perp})}{T(x)}\right) \\ &\times \exp\left(\frac{\mu(x) - m_T \cosh(y - \eta) \cosh \rho(r_{\perp})}{T(x)}\right). \end{aligned} \quad (5)$$

Before comparing with data we must still add the contributions from resonance decays. This is done following Refs. [11,12], again using thermal distributions (5) for the resonances. This procedure implies the assumption of full chemical equilibrium, including strange particles. As we will see this assumption is not very well justified, but sufficient for estimating resonance feeddown contributions. We only include resonances with masses up to the  $\Delta(1232)$  resonance. Tests showed that at the low freeze-out temperatures discussed below the inclusion of higher resonances has very little influence on the results.

At this point only  $T(x)$  and  $\mu(x)$  remain to be specified. The chemical potential of a hadron with baryon number  $B$  and strangeness  $S$  is fixed by the baryonic and strange chemical potentials as  $\mu(x) = B \cdot \mu_B(x) + S \cdot \mu_S(x)$  (we neglect small isospin asymmetry effects [13]). We have investigated two scenarios. In the first we set for simplicity  $T$ ,  $\mu_B$ , and  $\mu_S$  constant along the freeze-out hypersurface. In the second we select a Gaussian  $\eta$ -dependence of the freeze-out temperature,

$$T(\eta) = T_0 e^{-\left(\frac{\eta}{\Delta\eta}\right)^2}, \quad (6)$$

and fix  $\mu_B(\eta)$  by requiring freeze-out at constant baryon density. This is reasonable because in the range of  $T$  and  $\mu_B$  discussed below meson-meson reactions occur much

less frequently than meson-baryon or baryon-baryon reactions, making the baryon density the relevant control parameter for freeze-out. The strangeness chemical potential  $\mu_S$  is obtained as a function of  $T(\eta)$  and  $\mu_B(\eta)$  from the condition of local strangeness neutrality [13]. The thermal fit parameters in the model are thus  $\mu_B(\eta=0)$  and  $T_0$ , the baryon chemical potential and temperature at midrapidity, and the width  $\Delta\eta$  of the temperature profile (6).

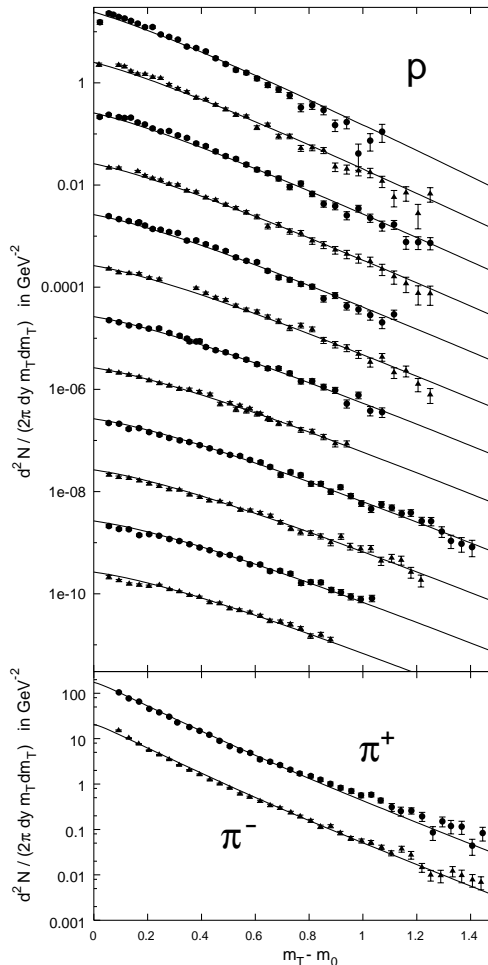


FIG. 1. Proton and pion  $m_T$ -spectra from E866 [3]. The proton spectra are given in rapidity bins of width 0.1; the top spectra correspond to  $0.5 \leq y_{\text{lab}} \leq 0.6$ , the bottom ones to  $1.6 \leq y_{\text{lab}} \leq 1.7$ . (Midrapidity is at  $y_{\text{lab}}=1.6$ .) Successive spectra are scaled down by a factor 10. The pion spectra are given for  $1.4 \leq y_{\text{lab}} \leq 1.6$ ; the  $\pi^-$  spectrum is divided by 10. Solid lines: best fit with Model 3.

Boost-invariant longitudinal flow combined with a cylindrical fireball geometry leads to nearly rapidity-independent transverse mass spectra near midrapidity. (For the present data midrapidity corresponds to  $y_{\text{lab}}=1.6$ .) This contradicts the measurements which show a clear rapidity dependence of the average transverse momentum  $\langle p_T \rangle$  and of the transverse slope parameters also near midrapidity, especially for the heavier

protons and  $\Lambda$ 's [3–5] (see also Figs. 1,2 and the discussion below). To describe the data one must therefore either reduce the transverse flow or the temperature as one moves away from midrapidity. Having investigated a wide range of possibilities, we here report on the results obtained by combining in various ways the following relatively simple options: Cylindrical (3) vs. elliptic (4) transverse geometry; constant vs.  $\eta$ -dependent (6) freeze-out temperature; and a constant ( $\rho(\eta)\equiv\rho_0$ ) vs. an  $\eta$ -dependent ( $\rho(\eta)=\rho_0\sqrt{1-(\eta^2/\eta_{\max}^2)}$ ) transverse flow gradient. The corresponding model parameters are listed in Table I.

symbol	description
$V \sim \tau_0 R_0^2$	fireball volume
$\eta_{\max}$	maximal longitudinal flow rapidity
$\rho_0$	maximal transverse flow rapidity
$\mu_B(\eta=0)$	baryon chemical potential at midrapidity
$T_0$	temperature at midrapidity
$\Delta\eta$	width of the longitudinal temperature profile

TABLE I. Model parameters. Note that  $\tau_0$  and  $R_0$  can be scaled out from the integrals in (5), leaving only the combination  $\tau_0 R_0^2$  as an independent fit parameter. It is proportional to the Lorentz invariant proper fireball volume  $V = \int_{\Sigma_f} u^\mu d\sigma_\mu$  which is quoted in Table II.

*Model 1* combines cylindrical geometry with constant temperature and transverse flow; as already mentioned it does not produce a very good fit. The parameters corresponding to the smallest  $\chi^2/\text{DOF}$  are listed in the first column of Table II. The quoted value of  $\chi^2/\text{DOF}=6.64$  was obtained after allowing for different overall normalizations for the various particle species than predicted by chemical equilibrium [14]. The corresponding normalization factors  $\mathcal{N}_i$  are also given; their deviation from 1 indicates the departure from chemical equilibrium at the point of thermal freeze-out. Effects of up to 25% are seen and should be expected in view of the finding in [15,16,9] that chemical freeze-out at the AGS occurs already at  $T_{\text{chem}} \simeq 130$  MeV.

Model 1 fails in two characteristic ways: (1) The rapidity spectra for heavy particles are too flat near midrapidity and too steep near  $y = \pm\eta_{\max}$ . (2) The slopes of the  $m_T$ -spectra are essentially constant in the region  $|y| \leq \eta_{\max}$  while the data show a significant steepening of the spectra already closer to midrapidity. Both failures are due to the boost-invariance of Model 1 in the region  $|\eta| \leq \eta_{\max}$ .

Due to the well-known weak sensitivity of the rapidity spectra to changes in the temperature [7] it is hard to improve on them by simply allowing the freeze-out temperature to depend on  $\eta$ ; with the parametrization (6) we found it to be impossible. A smooth reduction of the effective transverse flow as described above works much better, in particular if the simultaneous improvement on

the rapidity dependence of the transverse slopes is taken into account. Nevertheless, the proton and  $\Lambda$  rapidity distributions are still a bit too flat in the middle and too steep at the edges.

parameter	Model 1	Model 2	Model 3
$V/(10^4 \text{ fm}^3)$	1.74	1.74	1.82
$\eta_{\max}$	1.05	1.66	1.71
$\rho_0$	0.726	0.793	0.792
$\mu_B(\eta=0)/\text{MeV}$	548	549	536
$T_0/\text{MeV}$	90.5	91.6	93.3
$\Delta\eta$	$\infty$	$\infty$	3.58
$\mu_S(\eta=0)/\text{MeV}$	61.1	62.7	59.5
$\langle v_\perp \rangle(\eta=0)$	0.449	0.484	0.483
$\mathcal{N}_{\pi^+}$	0.924	0.920	0.920
$\mathcal{N}_{\pi^-}$	1.101	1.090	1.078
$\mathcal{N}_{K^+}$	1.218	1.239	1.268
$\mathcal{N}_{K^-}$	0.887	0.915	0.914
$\mathcal{N}_p$	0.972	0.978	0.972
$\mathcal{N}_\Lambda$	1.115	1.078	1.206
$\chi^2/\text{DOF}$	6.64	3.16	2.40

TABLE II. Fit results for the different models (see text for their description).

Surprisingly, a very good fit of both the rapidity and all the  $m_T$ -spectra can be obtained by simply reducing the transverse size of the fireball according to (4), without changing the freeze-out temperature or transverse flow gradient (*Model 2*). The reduced transverse radius in backward and forward rapidity regions not only leads to a faster and smoother decrease of the proton and  $\Lambda$  rapidity distributions, but the implied reduced *average* transverse flow away from midrapidity allows for an excellent fit to the steepening  $m_T$ -spectra. Combining Eq. (4) with an  $\eta$ -dependence of the transverse flow gradient overdoes it: the rapidity spectra become too sharply peaked near midrapidity. Some further fine-tuning of Model 2 is possible by combining the elliptic geometry (4) with an additional  $\eta$ -dependence of the freeze-out temperature (*Model 3*). However, the temperature gradients resulting from the fit are small, i.e. the width  $\Delta\eta \gg \eta_{\max}$  is large. In spite of the considerable expense in computing time resulting from the introduction of the additional parameter  $\Delta\eta$  its effect on  $\chi^2/\text{DOF}$  is only minor.

In Figures 1–3 we compare the results of Model 3 with the data; the corresponding curves from Model 2 would have been hardly distinguishable. Remaining minor flaws of Model 3 are a slightly too broad rapidity spectrum and somewhat too flat  $m_T$ -spectra in the very backward region for protons and a slight lack of curvature in the  $m_T$ -spectra for pions. Additional pion  $m_T$ -spectra covering the backward rapidity region  $0.6 < y_{\text{lab}} < 1.4$  have recently become available [17]; although we did not include them in our fit they agree with the predictions of our Model 3. Indeed, the lack of concavity of our calcu-

lated pion  $m_T$ -spectra becomes less of a problem at backward rapidities.

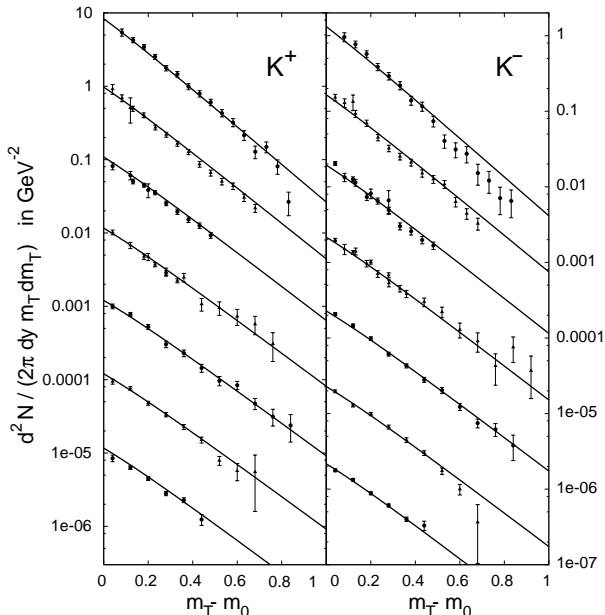


FIG. 2. Kaon  $m_T$ -spectra from E866 [3], in rapidity bins of width 0.2. Successive spectra are scaled down by a factor 10. The top spectra correspond to  $0.6 \leq y_{\text{lab}} \leq 0.8$ , the bottom ones to  $1.8 \leq y_{\text{lab}} \leq 2.0$ . Solid lines: best fit with Model 3.

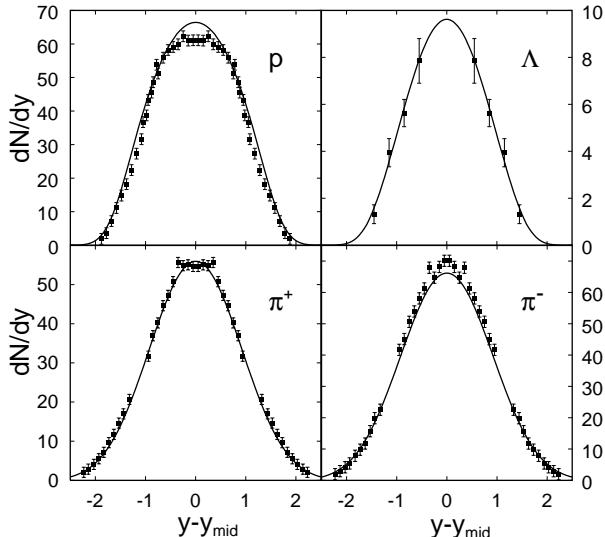


FIG. 3. Rapidity spectra of protons,  $\Lambda$  hyperons and pions in Au+Au collisions at the AGS. The  $\Lambda$ 's were measured by E891 [5]. For protons and pions we use data from E866 [3] near midrapidity and from E877 [4] for forward rapidities. The measured data points were reflected about midrapidity using the symmetry of the collision system. Solid lines: best fit with Model 3.

It is interesting to note that the thermal parameters, including the average radial flow velocity  $\langle v_{\perp} \rangle$ , are quite stable against the discussed variations in the model

parametrization [18]. Our analysis thus strongly suggests an average kinetic freeze-out temperature of about 90 MeV and an average radial flow velocity at midrapidity close to  $0.5c$ . Similarly low kinetic freeze-out temperatures were found in [10] for the smaller Si+Au system, in a model which has many similarities with ours. However, the analysis of [10] also included information from two-particle Bose-Einstein correlations which were not available for our system. The average transverse flow velocity at midrapidity in Si+Au is a bit smaller: with a linear transverse *velocity* profile Chapman and Nix [10] found  $\langle v_{\perp} \rangle(\eta = 0) = \frac{2}{3} \times (0.683 \pm 0.048) c \approx 0.45 c$ .

In [9] a successful fit of the rapidity spectra for pions, kaons, protons and  $\Lambda$ 's with a freeze-out temperature of 130 MeV was reported. The rapidity spectra are, however, not very sensitive to the freeze-out temperature [7]; we found that the large body of  $m_T$ -spectra are badly fit with  $T = 130$  MeV and clearly point to a considerably lower kinetic freeze-out temperature. On the other hand, the thermal freeze-out parameters found here correspond to a hadron resonance gas with an entropy per baryon  $S/A \simeq 12-13$ . This is the same range as found in the chemical freeze-out analysis of Si+Au collisions at the AGS [15] and confirmed later in Refs. [16,9,19] also for Au+Au collisions. Our findings are therefore consistent with chemical freeze-out at  $T_{\text{chem}} \approx 130$  MeV, followed by isentropic (hydrodynamic) expansion and kinetic freeze-out at  $T_{\text{kin}} \approx 90$  MeV.

Naively one would expect that increasing beam energy leads to higher energy deposition in the reaction zone and thus to higher temperature and/or stronger radial flow at freeze-out. A tendency for stronger flow at larger  $\sqrt{s}$  is indeed seen at energies below and including the AGS [20,21]. At the higher SPS energy an analysis of negative particle spectra and two-particle correlations from the NA49 Pb+Pb experiment points to kinetic freeze-out at  $T=100-120$  MeV with  $\langle v_{\perp} \rangle=0.45-0.5c$  [22,23], the lower freeze-out temperature and larger flow being preferred [23]. This supports our expectation, but contradicts an earlier analysis [24,20] which did not differentiate between chemical and kinetic freeze-out and thus gave larger freeze-out temperatures and smaller flow velocities.

We thank J.P. Wessels and C.A. Ogilvie for kindly sending us their data files, and J. Rafelski for a very constructive remark. We gratefully acknowledge the support of this work by BMBF, DFG and GSI.

[1] U. Heinz and B.V. Jacak, Ann. Rev. Nucl. Part. Sci. 49 (1999), in press (nucl-th/9902020).

[2] J. Harris and B. Müller, Ann. Rev. Nucl. Part. Sci. 46

- (1996) 71.
- [3] Y. Akiba et al. (E802 Coll.), Nucl. Phys. A 610 (1996) 139c; L. Ahle et al. (E802 Coll.), Phys. Rev. C 57 (1998) R466; and Phys. Rev. C 58 (1998) 3523.
  - [4] R. Lacasse et al. (E877 Coll.), Nucl. Phys. A 610 (1996) 153c.
  - [5] S. Ahmad et al. (E891 Coll.), Phys. Lett. B 382 (1996) 35.
  - [6] F. Cooper, G. Frye, Phys. Rev. D 10 (1974) 186.
  - [7] E. Schnedermann, J. Sollfrank, U. Heinz, Phys. Rev. C 48 (1993) 2462.
  - [8] J.D. Bjorken, Phys. Rev. D 27 (1983) 140.
  - [9] J. Stachel, Nucl. Phys. A 610 (1996) 509c.
  - [10] S. Chapman, J.R. Nix, Phys. Rev. C 54 (1996) 866; J.R. Nix, Phys. Rev. C 58 (1998) 2303.
  - [11] J. Sollfrank, P. Koch, U. Heinz, Phys. Lett. B 252 (1990) 256; and Z. Phys. C 52 (1991) 593.
  - [12] R. Venugopalan, Ph.D. thesis, SUNY Stony Brook, 1992.
  - [13] J. Letessier et al., Phys. Rev. C 51 (1995) 3408; P. Braun-Munzinger, I. Heppe, J. Stachel, nucl-th/9903010.
  - [14] For reasons of stability of the fit the normalization constants  $\mathcal{N}_i$  were determined after fitting the thermal parameters, by minimizing the  $\chi^2$  of the corresponding spectrum  $i$  keeping the other parameters fixed. This procedure is justified as long as the  $\mathcal{N}_i$  are sufficiently close to 1 such that resonance feeddown is not seriously affected. Without separately optimized normalization factors the best fit with Model 1 gives  $\chi^2/\text{DOF} = 8.04$ .
  - [15] J. Letessier, J. Rafelski, A. Tounsi, Phys. Lett. B 328 (1994) 499.
  - [16] P. Braun-Munzinger et al., Phys. Lett. B 344 (1995) 43.
  - [17] L. Ahle et al. (E802 Coll.), Phys. Rev. C 59 (1999) 2173.
  - [18] For ellipsoidal freeze-out geometry the temperature and the average radial flow velocity at midrapidity are somewhat higher than for a cylindrical fireball; once averaged over rapidity, the values are, however, quite similar.
  - [19] J. Cleymans, K. Redlich, nucl-th/9903063 (Fig. 4).
  - [20] N. Herrmann, Nucl. Phys. A 610 (1996) 49c.
  - [21] R. Seto et al. (E917 Coll.), Nucl. Phys. A 638 (1998) 407c.
  - [22] H. Appelshäuser et al. (NA49 Coll.), Eur. Phys. J. C 2 (1998) 661.
  - [23] B. Tomášik, PhD Thesis, Regensburg, 1999, and to be published. The quoted values were obtained for rapidities  $1 \leq y - y_{\text{cm}} \leq 1.5$ , i.e. not at midrapidity. The spectra and correlations and midrapidity [22] appear to require even larger radial flow velocities.
  - [24] P. Braun-Munzinger et al., Phys. Lett. B 365 (1996) 1.